

Molecular Docking of Secondary Metabolite Compounds of *Andrographis paniculata* Plant as Potential Covid-19 Drug Candidate

Netty Ino Ischak, Akram La Kilo*, Dandi Saputra Halidi, La Ode Aman, Jafar La Kilo, Weny J.A. Musa

Study Program of Chemistry, Faculty of Mathematics and Natural Sciences, Universitas Negeri Gorontalo, Gorontalo, Indonesia

*Email Korespondensi: akram@ung.ac.id

Abstract

The aim of this research was to investigate the interaction between secondary metabolite compounds and the Mpro receptor, which was the main protein in Covid-19. Ligand-receptor interactions were studied using the molecular docking method. The validation results indicated that the test ligand andrographolide had a higher affinity value compared to the standard ligand, with a value of -6.6 kcal/mol compared to the standard ligand's -7.5 kcal/mol. Additionally, the compound 14-Acetyl-3,19-isopropylideneandrographolide, 5,4 dihydroxy-7,8,2',3'-tetramethoxyflavone-5-glucoside had an affinity of -7.5 kcal/mol, andrographidin A had -7.6 kcal/mol, andrographiside had -7.7 kcal/mol, skullcapflavone I had 7.7 kcal/mol, 5-hydroxy-7,8,2'-trimethoxyflavone-5-glucoside had -7.7 kcal/mol, apigenin had 7.7 kcal/mol, 5-hydroxy-7,8-dimethoxyflavone-5-glucoside had -7.8 kcal/mol, neoandrographolide had -7.8 kcal/mol, andropanoside had -7.9 kcal/mol, wogonin-5 glucoside had -8.1 kcal/mol, 5,2',3'-Trihydroxy-7,8-dimethoxyflavone-3'-glucoside had -8.4 kcal/mol, and bisandrographolide had -8.5 kcal/mol. From the molecular docking results, the secondary metabolite compounds from the *Andrographis paniculata* plant exhibited significant interactions surpassing the standard ligand N3. Active residue interactions observed included Phe140, Leu141, Asn142, Gly143, His163, Glu166, Gln189, and Thr190.

Keywords: *Andrographis paniculata*; Covid-19 drug; Mpro receptor; molecular docking

Received: 25 May 2023

Accepted: 31 May 2023

DOI: <https://doi.org/10.25026/jsk.v5i3.1845>



Copyright (c) 2023, Jurnal Sains dan Kesehatan (J. Sains Kes.).
Published by Faculty of Pharmacy, University of Mulawarman, Samarinda, Indonesia.
This is an Open Access article under the CC-BY-NC License.

How to Cite:

Ischak, N.I., La Kilo, A., Halidi, D.S., Aman, L.O., La Kilo, J., Musa, W.J.A., 2023. Molecular Docking of Secondary Metabolite Compounds of *Andrographis paniculata* Plant as Potential Covid-19 Drug Candidate. *J. Sains Kes.*, 5(3). 324-338. DOI: <https://doi.org/10.25026/jsk.v5i3.1845>

1 Introduction

Covid-19, or coronavirus disease, was the name of the disease that was spreading at the time. Meanwhile, SARS-CoV-2 was the name of the virus that caused covid-19. The naming of SARS-CoV-2 was due to its identification as a novel variant of the coronavirus, which had caused the severe acute respiratory syndrome (SARS) outbreak in 2002-2003. As a result, this virus was named severe acute respiratory syndrome-related coronavirus 2 or SARS-CoV-2. Coronavirus (CoV) was a genus within the Coronaviridae family, named after the crown-like spikes found on its surface. They were a large family of viruses that had the largest RNA genomes among all RNA viruses. This genome acted as an RNA messenger during cell infection, directing the synthesis of two polyproteins that encompassed the machinery necessary for the replication of new viruses. SARS-CoV-2 belonged to the coronavirus family, with a single-stranded RNA as its genetic material. It had shown a high similarity to other coronaviruses, including SARS. Covid-19, caused by the SARS-CoV-2 virus, was classified as a β -coronavirus and represented an acute respiratory disease that infected humans, for which humans did not possess a natural immune defense against this pathogen [1].

The philosophy of drug discovery has transformed from "one drug, one target" to "one drug, multiple targets" paradigm. Secondary metabolites derived from plants held potential multi-targeting properties because they needed to undergo defense mechanisms developed by plants against predators such as bacteria, fungi, and viruses. *A. paniculata* Burm.f. Nees, commonly known as *sambiloto*, was a medicinal plant with significant pharmaceutical value due to its antiviral and anti-inflammatory properties

[2]. It exhibited antiviral and anti-inflammatory properties and had been referred to as a miraculous remedy since the Spanish Flu pandemic in 1918 for inhibiting the growth or spread of viruses [2]. Medicinal plants have been used as folk remedies for centuries for diseases now known to be of viral origin [3].

There is an increasing need for the search of new compounds with antiviral activity as the treatment of viral infections with the available antiviral drugs is often unsatisfactory due to the problem of viral resistance coupled with the problem of viral latency and conflicting efficacy in recurrent infection in immunocompromised patients [3]. Ethnopharmacology provides an alternative approach for the discovery of antiviral agents, namely the study of medicinal plants with a history of traditional use as a potential source of substances with significant pharmacological and biological activities [3]. Many medicinal plants have been demonstrated to possess various antiviral activities against different viruses [4]. *Sambiloto* has been shown to have potential medicinal properties, including anticancer, antidiabetic, and immunomodulatory effects [5]–[9].

Drug repurposing was commonly employed in the search for potential therapeutic agents. *A. paniculata*, a medicinal plant commonly used to alleviate symptoms of common flu, and its phytoconstituent andrographolide, had repeatedly been identified as potential antiviral agents against SARS-CoV-2 [10]. Considering the emerging evidence since the onset of the Covid-19 pandemic, this rapid review was conducted to identify and evaluate the current antiviral evidence of *A. paniculata*, andrographolide, and its analogs against SARS-CoV-2. Even so, it has not been disclosed which ligands in *sambiloto*

can inhibit Covid-19, especially in the Mpro receptor. This study described 15 out of 36 ligands that were evaluated on sambiloto (*Andrographis paniculata*), which interacted with the Mpro receptor and had potential as anti-COVID-19 candidates. The evaluation was performed using the molecular docking method. Molecular docking, or molecular docking analysis, was a computational method aimed at predicting the binding interactions between a macromolecule (target) and a small molecule called a ligand, which bound non-covalently [11]–[13]. This research utilized in silico molecular docking method. In silico studies integrated experimental chemical knowledge based on mathematical algorithms, statistics, and databases. This method could also serve as an initial study that supported in vitro and in vivo experimental research.

2 Methods

2.1 Research tools and materials

The equipment used in this research consisted of hardware and software. The hardware used was a toshiba satellite M840 laptop with an intel® core(TM) i5-3210M CPU @2.50 GHz processor, equipped with 12 GB of Random Access Memory (RAM) and 120GB SSD & 512 GB HDD internal memory. The computer operated on the windows 10 Pro operating system. The software used included chem 3D professional version 15.0, discovery studio 2021 client, AutoDock, and AutoDock Vina version 1.5.6, which were produced by the Scripps Research Institute. PyMOL and PyRx were also utilized.

The materials used in this research consisted of secondary metabolite compounds derived from the sambiloto plant, which were obtained and downloaded directly from the PubChem compound website in a three-dimensional structure format (.sdf). The macromolecule utilized was a crystal structure of the receptor protein obtained from the Protein Data Bank (PDB) with the corresponding macromolecule code (PDB ID: 6LU7) available on the www.rcsb.org, as shown in figure 1.

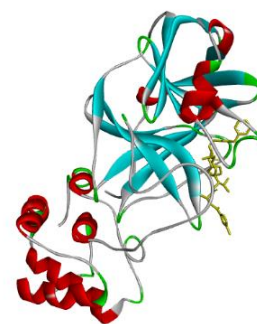


Figure 1 Structures of protein and N3 inhibitor

2.2 Research Procedure

2.2.1 The structure and geometry optimization of the andrographolide compound.

The structure of secondary metabolite compounds from the *sambiloto* plant could be downloaded from the webpage on the PubChem compound website (<https://pubchem.ncbi.nlm.nih.gov>) in three-dimensional format and saved as .sdf files. Subsequently, the downloaded compound structures underwent a geometry optimization process using the chem 3D professional program and the molecular mechanics (MM2) method, repeated 1000 times to obtain stable conformational structures. The obtained conformational results were then saved in .pdb format.

2.2.2 The downloading of the target macromolecule

The macromolecule utilized in this research was obtained from the RCSB Protein Data Bank website with the ID (PDB ID: 6lu7) in .pdb format.

2.2.3 Removing water molecules from the macromolecule

The macromolecule structure that had been downloaded in .pdb format was opened using the discovery studio 2021 client program by selecting file → open (Ctrl + O). Then, water molecules were removed from the anti-cancer macromolecule by going to the script → selection → select water Molecules menu and pressing the delete key on the keyboard.

2.2.4 Separation of macromolecule chains

The three-dimensional structure of the downloaded macromolecule contained chains or ligands attached to the macromolecule. Using the discovery studio 2021 client program, the attached ligands or chains were separated from the macromolecule. This separation resulted in a macromolecule without chains or ligands and ligands without the macromolecule structure. After the separation, both were saved in .pdb format.

2.2.5 Preparation of the macromolecule for target docking

The macromolecule, which had been separated from the chains or ligands, underwent preparation by adding hydrogen atoms to each residue at the ends of the macromolecule using the AutoDock Tools program version 1.5.6. Subsequently, partial charges were assigned to the macromolecule using the same program. Finally, the macromolecule with added hydrogen atoms and partial charges was saved in .pdbqt format.

2.2.6 Determining the grid box

The macromolecule, which had hydrogen atoms added to the residue ends and partial charges assigned, underwent the determination of the Grid Box size based on the native ligand previously bound to the macromolecule. This was done by opening and selecting the ligand that had been separated from the macromolecule in the program to determine the size of the grid box, using spacing in angstrom units [14].

2.2.7 Redocked the native ligand to the macromolecule

Before performing the Docking Simulation, the docking method used was validated by redocking or re-docking the native ligand to the macromolecule [15]. Docking validation was done by determining the Root Mean Square Deviation (RMSD) value. The redocking process was considered successful if the RMSD value was less than 2.0 Å [12], [16]. The redocking process was performed using the AutoDock Vina program version 1.5.6.

2.2.8 Docked the Test Ligand to the Macromolecule

The docking of the chloroquine test ligand was performed using the AutoDock Vina 1.5.6 program through the Command Prompt. The coordinate values or positions of the grid box used were the same as the grid box size for the native ligand docked to the target macromolecule, with predefined values for center_x, center_y, and center_z. The program calculated and calculated the scoring values for the test ligand docked to the macromolecule [17].

2.2.9 The docking results analysis

The docking results were then visualized using the PyMOL and LigPlus programs. The data obtained from the docking results included the scoring values of the binding free energy (ΔG) for the ligands bound to the macromolecule. The more negative the binding value between the ligand and the receptor, the higher the effectiveness of the ligand as an anticancer candidate. By using the PyMOL and LigPlus programs, the interactions formed between the ligands and the receptor could be visualized in two-dimensional and three-dimensional representations.

3 Results and Discussions

The Literature Review was initiated with the keyword "Covid-19," referring to various references for docking simulations of Covid-19 drug compounds. The screening process of these references resulted in the identification of the protein structure 6LU7, which had been extensively studied. This protein structure was then combined with secondary metabolites from the *sambiloto* plant (*A. paniculata*), which were commonly used by chemistry students as an herbal drink during orientation activities. The source of this plant study was [18], who investigated the clinical activities of *sambiloto* leaves as a traditional medicine for anti-inflammatory and cold remedies.

The selection of the protein 6LU7 as the receptor in this research was based on its role as the main protease enzyme (Mpro) that actively mediated replication and transcription in the SARS-CoV-2 virus [19]. Prior to conducting molecular docking studies on the secondary metabolites of *sambiloto* (*A.*

paniculata), the 6LU7 receptor was redocked using its original ligand (inhibitor N3) as a positive control to validate the molecular docking method. The stages of this research included the preparation and optimization of the protein-ligand structure, followed by the Molecular Docking phase, which involved analyzing the Root Mean Square Deviation (RMSD) values, binding energy (ΔG), and the number of interactions or bonds formed between the protein and ligand.

3.1 Preparation and optimization of protein and ligand structures.

Preparation and optimization were necessary to obtain protein and ligand structures in their optimal state, ensuring stability and conformity with their natural conformation. This stage aimed to acquire three-dimensional structures of proteins and ligands that would be used in the Molecular Docking simulation process. Generally, not all available protein and ligand structures were in their natural state. Therefore, preparation and optimization were required before utilizing them in silico processes to test and determine antiviral activity and evaluate their potential as Covid-19 candidate drugs.

3.2 Preparation and optimization of Covid-19 glycoprotein structure.

Protein Mpro, which was found in Covid-19, could be obtained from the protein data bank with the code 6LU7 as shown in figure 2, accessed through the website <http://www.rcsb.org/pdb>, along with the inhibitor N3.

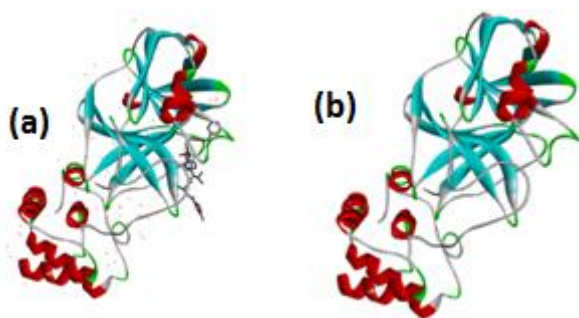


Figure 2: 3-D Structure of Mpro Covid-19 Protein (PDB code: 6lu7) before (a) and after (b) preparation.

Figure 2 displayed the three-dimensional structure of the Mpro protein, visualized using the discovery studio visualizer application, version 2021. The subsequent step involved separating the native ligand bound to the Mpro protein and removing all solvent molecules, specifically water molecules. The separation of the native ligand from the protein was performed with the aim of replacing the position of the native ligand with a test ligand, which would be used as a comparative or standard ligand during the process of molecular docking and molecular dynamics. Ligands that were still bound to the protein's active site hindered and occluded other ligands from entering and interacting with the amino acid residues in the protein molecule. Therefore, it was necessary to separate the ligand from the protein macromolecule that would be the target for molecular docking.

The next step involved optimizing the protein by adding hydrogen atoms to the ends of the amino acid residues in the Mpro Covid-19 protein and applying Gasteiger Charges as partial charges to the cleaned Mpro Covid-19 protein, devoid of ligands and solvent molecules, using the AutodockTools software. The addition of hydrogen atoms to the protein was only performed for polar hydrogen atoms. This was because polar hydrogen atoms had the potential to form bonds with ligands and could influence molecular interactions during the simulation process.

3.3 Preparation and optimization of test ligands

The ligand compounds used in this study were secondary metabolites from the *A. paniculata* plant and standard ligands that had formed complexes with the Mpro protein. The standard ligands were obtained from PubChem compound, which could be accessed through <https://pubchem.ncbi.nlm.nih.gov>. This website served as a database archive that provided various structures and molecular compounds found in nature in three-dimensional form, storing them in .sdf file format. On the other hand, the ligands or secondary metabolite compounds from the *A. andrographis paniculata* plant could be viewed on KNApSACK-ID, accessed through http://knapsack3d.sakura.ne.jp/all.php?select=Organism&search_key=Andrographis+panicul

ata and then downloaded using PubChem. The available ligand structures on the PubChem Compound page were generally not optimized, and their structures were still in an unstable form and had a high energy. The energy minimization and geometry optimization of the ligand structures were performed using the PyRex application with the assistance of the OpenBabel tool, and they were visualized using the discovery studio visualizer application.

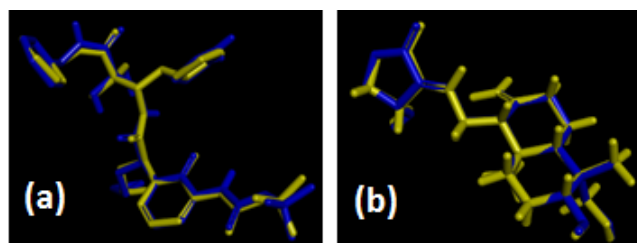


Figure 3: 3D structure of standard ligand (a) and andrographolide (b) before (blue) and after optimization (yellow).

3.4 Molecular Docking

After obtaining the protein and ligand structures through the preparation and optimization steps, the next step was to perform molecular docking simulations. Molecular docking was conducted by docking the ligand to the active site (binding site) of the Mpro Covid-19 protein. The molecular docking stage included determining the grid box, validating docking, docking the test ligand to the protein, and analyzing and visualizing the docking simulation results.

3.5 Determination of the Grid Box

After obtaining the protein and ligand structures through the preparation and optimization steps, the next step was to perform molecular docking simulations. Molecular docking was conducted by docking the ligand to the active site (binding site) of the Mpro Covid-19 protein. The molecular docking stage included determining the grid box, validating docking, docking the test ligand to the protein,

and analyzing and visualizing the docking simulation results.

The determination of the grid box involved modifying the size of the grid box using the AutodockTools program. The grid box represented the spatial location for ligand binding on the protein. The size of the grid box was adjusted using Angstrom (\AA) units to limit the search for ligand conformations during the ligand docking process on the protein. The grid box size was based on the position of the native ligand that had bound to the active site, with the grid center centered on the native ligand and a spacing of 1.0 \AA to ensure the ligand was within the grid box. In this study, the grid box size used for the Mpro Covid-19 protein binding site was x, y, and z, with values of -10.729204 , 12.417653 , and 68.816122 \AA , respectively, resulting in a grid box volume of $10 \times 22 \times 16$ Angstrom.

3.6 Docking method validation

The docking method validation involved redocking the standard ligand, which had previously bound to the active site of the Mpro-Covid19 protein, using the Pyrex program with the Vina Wizard tool (Autodock Vina). The redocking process served as a reference for the test ligand and aimed to observe the receptor-ligand interactions of the Mpro protein from Covid-19. During this process, molecular docking was also performed with the secondary metabolite compounds from the *A. paniculata* with the Mpro receptor, estimated to take approximately 14 hours. The success rate of the docking simulation was assessed based on the binding affinity, which was determined by the binding free energy (ΔG) between the ligand and receptor molecules. Binding affinity served as a measure of the ligand's ability to bind to the receptor, with lower binding values indicating higher affinity between the receptor and ligand, and conversely, higher binding affinity indicating lower affinity.

Among the 36 test ligands, each with 10 conformations, the best conformation and the binding affinity value that met or closely approximated the standard ligand were selected as shown in table 1.

Table 1. Binding energy of molecular docking results between ligands and Mpro receptor.

Ligands	Binding Affinity (kcal/mol)	Hydrogen Bond	Distance (Å)
Standard ligand	-7.5	O-Glu166	2.74
		HN--Gln189	2.24
		HN-Glu166	2.50
		HN-Phe140	2.63
Andrographolide	-6.6	H-Arg105	2.13
		O-Gln110	2.83
		H-Thr111	2.84
		H-Asp295	2.93
		H-Thr169	2.82
Bisandrographolide	-8.5	O-Arg131	2.82
		O-Asn238	2.90
		O-Thr199	2.94
		H-Asp187	2.15
Apigenin	-7.7	H-Ser144	2.67
		H-Tyr54	2.70
		H-His163	2.91
5-Hydroxy-7,8-dimethoxyflavone_5-glucoside	-7.8	H-Leu141	2.09
Andrographidin A	-7.6	H--Ser144	2.21
		H--Leu141	2.68
Andropanoside	-7.9	H--Leu141	2.91
		O-Gly143	3.02
		H-His163	2.57
		H-Thr26	2.65
		H-Thr25	2.87
		H-Thr45	2.95
		O-Gly143	3.06
		O-Ser144	3.19
		O-Ser144	3.21
		O-Gly143	3.21
5,2',3'-Trihydroxy-7,8-dimethoxyflavone-3'-glucoside	-8.4	H-Leu141	2.46
		H-Ser144	2.54
		O-Gln192	3.19
		O-Ser144	3.23
5,4-Dihydroxy-7,8,2',3'-tetramethoxyflavone-5-glucoside	-7.5	H-Thr190	1.97
		O-Gln192	3.05
Wogonin-5-glucoside	-8.1	H-Leu141	1.73
		H-Ser144	2.30
		H-Thr26	2.51
		H-Thr26	.286
		O-Cys145	3.37
5-Hydroxy-7,8,2'—trimethoxyflavone-5-glucoside	-7.7	H-His163	2.56
		H-Asn142	2.71
		H-Leu141	2.80
		O-Gly143	3.25
		H--Leu141	2.05
Neoandrographolide	-7.8	H--Ser144	2.38
		H--Ser144	2.50
		O--Ser114	2.80
		O--Thr25	2.80
		O-Thr45	2.91
		O-Gly143	3.10
		O--Gly143	3.24
		H--Thr190	1.90
		H-Asn142	2.75
		O-Glu166	3.24
14-Acetyl--3,19-isopropylideneandrographolide	-7.5	O-Gln192	3.40
		O--Arg131	2.81
		O-Asn238	3.02
		O-Thr199	3.07
Andrographiside	-7.7	H-Leu287	2.10
		H-Leu271	2.40
		H-Asp243	2.43
		H-Thr199	2.47
		H-Asn238	2.52
		O-Lys137	3.19

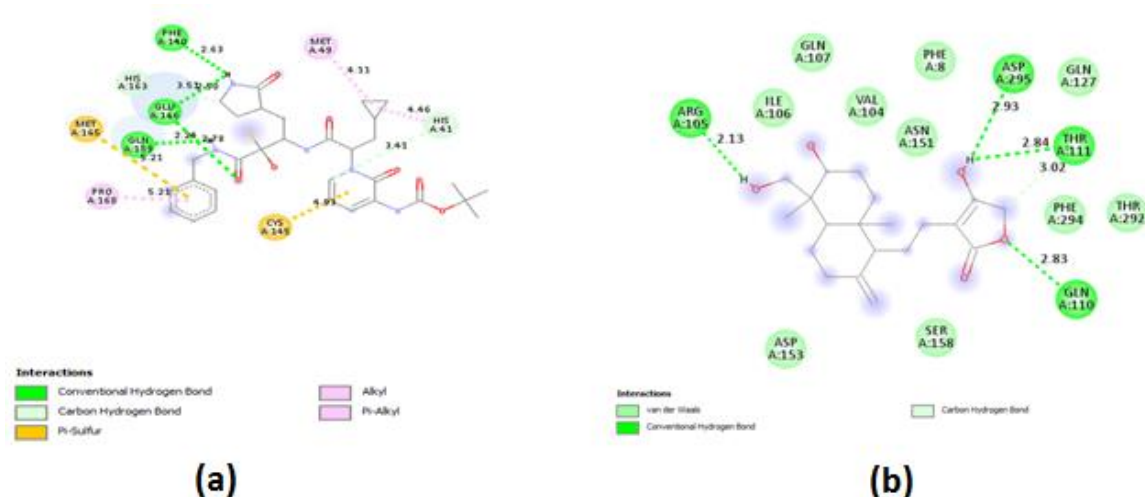


Figure 4. Visualization of 2D structures of the standard ligand (a) and andrographolide compound (b) along with their respective types of bonds.

Table 1 showed the formation of hydrogen bonds between both the standard ligand and the test ligand with the Mpro receptor of the Covid-19 protein, with varying numbers and distances.

3.7 Analysis of the docking results

The docking simulation results for each ligand on the Mpro protein provided diverse outcomes, with the best conformations for each ligand resulting in binding affinities that matched or even exceeded those of the standard ligand, despite the main compound, andrographolide, having lower affinity than its standard ligand. The analysis of the docking simulation results was based on the magnitude of the binding affinity, where lower affinity indicated a higher likelihood of the ligand being a candidate for Covid-19 treatment.

Hydrogen bonds were formed through the electrostatic interaction of hydrogen atoms covalently bonded to highly electronegative atoms such as O, N, and S as shown figure 4. The docking simulation results for the ligands showed hydrogen bonding interactions between the standard ligand and the receptor, specifically with Glu166 through an O atom bond at a distance of 2.74 Å, and with Gln189, Glu166, and Phe140 through NH groups at bond distances of 2.24 Å, 2.50 Å, and 2.63 Å, respectively, resulting in an affinity value of -7.5 kcal/mol. The affinity value served as the standard for the test ligands. Additionally, there

were several hydrophobic interactions involving His41, Met49, Cys145, His163, Met165, and Pro168 (figure 4).

The first test ligand was the primary secondary metabolite compound found in the *A. paniculata* plant, known as andrographolide. It formed a hydrogen bond with Gln110 through an O atom at a bond distance of 2.83 Å, and with Arg105, Thr111, and Asp295 at distances of 2.13 Å, 2.84 Å, and 2.93 Å, respectively. Its affinity value of -6.6 kcal/mol was higher than that of the standard ligand, indicating good interactions between the ligand and receptor involving both hydrogen bonding and hydrophobic interactions. However, it is worth noting that the viability of this compound for use as a treatment could not be solely determined based on these interactions.

14-Acetyl-3,19-isopropylideneandrographolide had hydrogen bonds with Arg131, Asn238, and Thr199 through O atoms at bond distances of 2.81 Å, 3.02 Å, and 3.07 Å, respectively (figure 5). It exhibited a similar binding affinity to the standard ligand, which was -7.5 kcal/mol. Similarly, for the ligand 5,4-dihydroxy-7,8,2',3'-tetramethoxyflavone-5-glucoside, the affinity value was also -7.5 kcal/mol. It had hydrogen bonds with Thr190 through an H atom and with Gln192 through an O atom at bond distances of 1.97 Å and 3.05 Å, respectively.

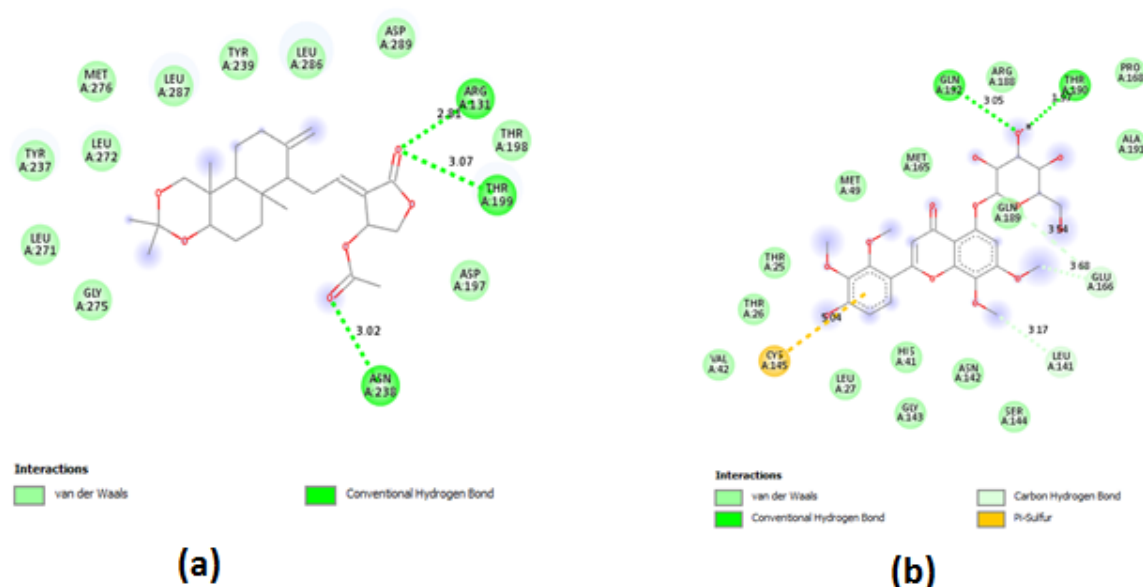


Figure 5. 2D of ligands: (a) 14-Acetyl-3,19-isopropylideneandrographolide and (b) 5,4-dihydroxy-7,8,2',3'-tetramethoxyflavone-5-glucoside.

Wogonin-5-glucoside formed hydrogen bonds with Leu141, Ser144, Thr26, and Thr26, binding to the H atom with bond distances of 1.73 Å, 2.30 Å, 2.51 Å, 2.86 Å, and 3.37 Å, respectively (figure 6a). Additionally, there was an H-O bond with Cys145 at a distance of 3.37 Å. This ligand exhibited an affinity value of -8.1. In the case of apigenin, hydrogen bonds were observed between Asp187, Ser144, Tyr54, and His163, binding to the H atom at bond distances of 2.15 Å, 2.67 Å, 2.70 Å, and 2.91 Å, respectively, resulting in an affinity value of -7.7 kcal/mol (figure 6b). 5-Hydroxy-7,8-dimethoxyflavone-5-glucoside formed hydrogen bonds with Leu141 and Ser144 at bond distances of 2.09 Å and 2.21 Å, respectively, with an affinity value of -7.8 kcal/mol (figure 6c). Andrographidin A, with an affinity value of -7.6 kcal/mol, formed hydrogen bonds with Leu141 at two different bond distances, 2.68 Å and 2.91 Å, and with Gly143 at a bond distance of 3.02 Å (figure 6d). Andropanoside formed hydrogen bonds with His163, Thr26, Thr25, and Thr45, binding to the H atom at bond distances of 2.57 Å, 2.65 Å, 2.87 Å, and 2.95 Å, respectively, and with Gly143 and Ser144 at bond distances of 3.06 Å and 3.19 Å, respectively, resulting in an affinity value of -7.9 kcal/mol (figure 6e). Finally, 5,2',3'-Trihydroxy-7,8-dimethoxyflavone-3'-glucoside formed hydrogen bonds with Leu141 and Ser144 at bond distances of 2.46 Å and 2.54 Å,

respectively, and with Gln192 and Ser144 at bond distances of 3.19 Å and 3.23 Å, respectively, with an affinity value of -8.4 kcal/mol (figure 6c).

Bisandrographolide (figure 7) had the lowest affinity, which was -8.5 kcal/mol. Hydrogen bonds were formed with Thr169, Arg131, Asn238, and Thr199, with bond distances of 2.82 Å, 2.82 Å, 2.90 Å, and 2.94 Å, respectively. 5-Hydroxy-7,8,2'-trimethoxyflavone-5-glucoside formed hydrogen bonds with His163, Asn142, and Leu141 at the H atom, with bond distances of 2.56 Å, 2.71 Å, and 2.80 Å, respectively, and with Gly143 at the O atom with a bond distance of 3.25 Å. The affinity value of the ligand 5-Hydroxy-7,8,2'-trimethoxyflavone-5-glucoside was -7.7 kcal/mol.

Similarly to 5-Hydroxy-7,8,2'-trimethoxyflavone-5-glucoside, there were two ligands with the same affinity value: Andrographiside and Skullcapflavone I (figure 8). Andrographiside formed hydrogen bonds between the H atom and Leu287, Leu271, Asp243, Thr199, and Asn238, with bond distances of 2.10 Å, 2.40 Å, 2.43 Å, 2.47 Å, and 2.52 Å, respectively, and between the O atom and Lys137, with a bond distance of 3.19 Å. As for Skullcapflavone I, hydrogen bonds occurred between Thr190 and Asn142, with bond distances of 1.90 Å and 2.75 Å, respectively.

Additionally, the O atom formed bonds with Glu166 and Gln192, with bond distances of 3.24 Å and 3.40 Å, respectively. Neoandrographolide, with an affinity value of -7.8, formed hydrogen bonds with the amino acids Leu141, Ser144, and Ser144 at the H atom, with bond distances of

2.05 Å, 2.38 Å, and 2.50 Å, respectively. At the O atom, hydrogen bonds occurred with Ser114, Thr25, Thr45, Gly143, and Gly143, with bond distances of 2.80 Å, 2.80 Å, 2.91 Å, 3.10 Å, and 3.24 Å, respectively.

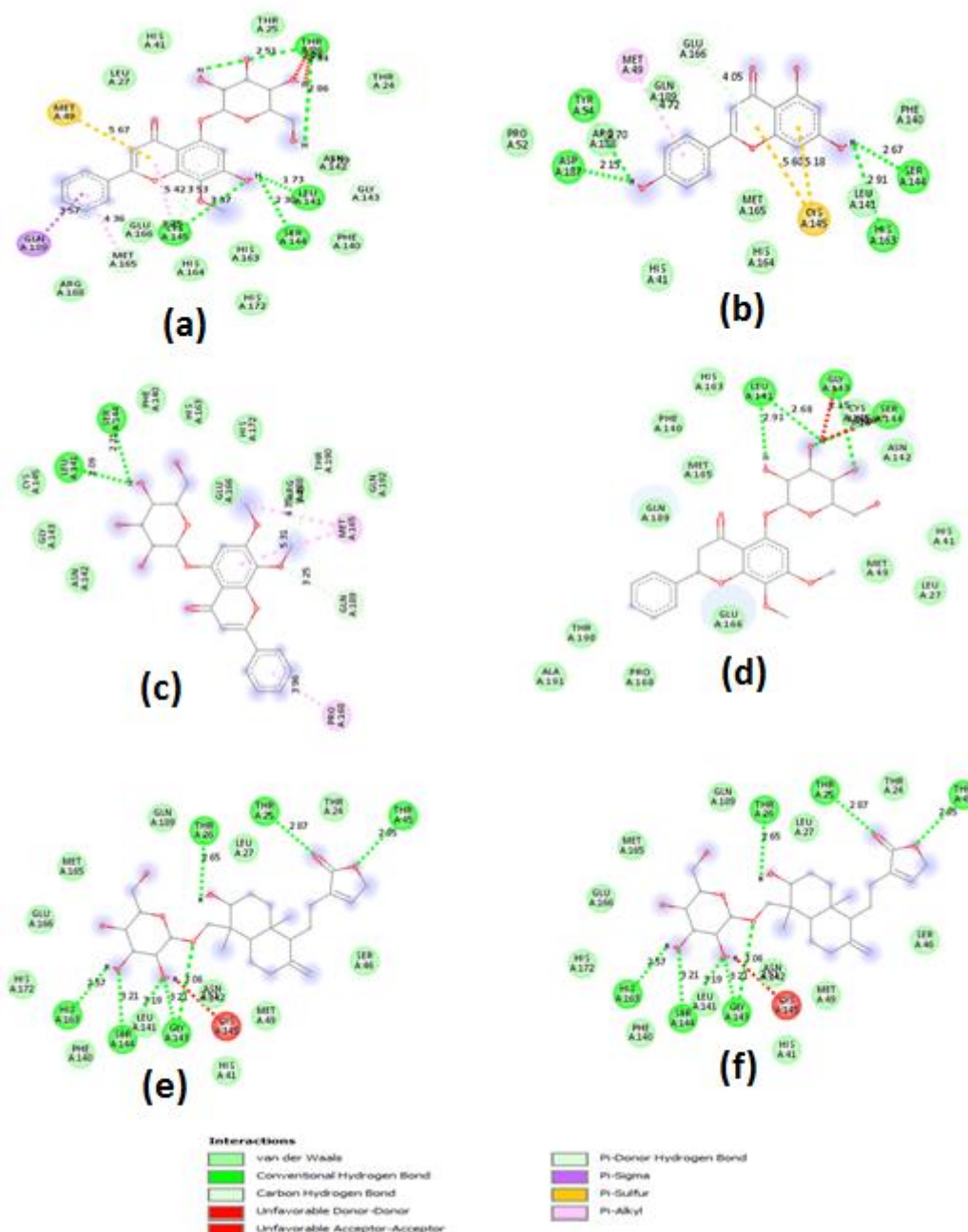


Figure 6. Types of bond: (a) Wogonin-5-glucoside, (b) Apigenin, (c) 5-Hydroxy-7,8-dimethoxyflavone-5-glucoside, (d) Andrographidin A, (e) Andropanoside, and (f) 5,2',3'-Trihydroxy-7,8-dimethoxyflavone-3'-glucoside.

Based on the search results, there is no direct evidence that the secondary metabolite compounds from the andrographis plant are capable of interacting with the Mpro protein of Covid-19. However, there are several studies that have investigated the potential of natural compounds to inhibit the Mpro protein of SARS-CoV-2, which causes Covid-19. These studies have used in-silico methods to identify potential candidates for drug development. Some of the compounds that have shown potential in these studies include sterols from sea fan [20], natural compounds with anticancer properties [21], ferruginol and trans-communic acid from *Papuacedrus papuana* [22], glycyrrhizin and 18- β -glycyrrhetic acid [23], and strawberry and ginger silver nanoparticles [24]. One study also investigated the binding affinity of andrographolide and its derivative with targets related to Covid-19 and their probable role in regulating multiple pathways in Covid-19 infection [25]. However, further research is needed to determine the effectiveness of these compounds in inhibiting the Mpro protein of SARS-CoV-2 in vivo.

Among the 14 best test ligands, Andrographolide, which is the main secondary metabolite compound from the andrographis plant, is the only ligand whose affinity value is greater than the standard ligand, which is -6.6 kcal/mol compared to the standard ligand's -7.5 kcal/mol. The other two ligands that have the same affinity value are 14-Acetyl-3,19-isopropylideneandrographolide and 5,4-dihydroxy-7,8,2',3'-tetramethoxyflavone-5-glucoside. The other test ligands have smaller affinity values than the standard ligand: Andrographidin A with -7.6 kcal/mol, Andrographiside with -7.7 kcal/mol, Skullcapflavone I with -7.7 kcal/mol, 5-Hydroxy-7,8,2'-trimethoxyflavone-5-glucoside with -7.7 kcal/mol, Apigenin with -7.7 kcal/mol, 5-Hydroxy-7,8-dimethoxyflavone-5-glucoside with -7.8 kcal/mol, Neoandrographolide with -7.8 kcal/mol, Andropanoside with -7.9 kcal/mol, Wogonin-5-glucoside with -8.1 kcal/mol, 5,2',3'-Trihydroxy-7,8-dimethoxyflavone-3'-glucoside with -8.4 kcal/mol, and Bisandrographolide with -8.5 kcal/mol, which is the ligand with the smallest affinity value. Therefore, these 14 ligands can be

considered as potential candidates for Covid-19 drugs.

A recent study evaluated the in silico (molecular docking) properties of active compounds available in *Orthosiphon stamineus* Benth (OS) and compared its effect with remdesivir and favipiravir as positive compounds based on docking properties [26]. The results showed that most of the studied main compounds perform better than selected drugs in inhibition of the spike protein in Covid-19. According to the combined scores in binding affinity, the drug-likeness properties of the ligand, andrographolide, revealed to be the best possible Covid-19 inhibitor as compared to the other ligands [26].

Another study investigated the therapeutic efficacy of eight withanolides (derived from *Ashwagandha*) against the angiotensin-converting enzyme 2 (ACE2) proteins, a target cell surface receptor for SARS-CoV-2 [27]. Among all withanolides, Withaferin-A, Withanone, Withanoside-IV, and Withanoside-V significantly inhibited the ACE2 expression [27]. A study evaluated the inhibitory potency of *Ashwagandha* withanolides and its aqueous extracts against ACE2 [27]. The results showed that stem-derived extracts had a higher ACE2 inhibitory potency than leaf-derived extracts [27].

Another study applied a bioinformatics approach including molecular docking and a combination of molecular dynamics simulations and Poisson-Boltzmann surface area (MM/G/P/BSA) free energy calculations to identify the inhibitory potency of candidates against SARS-CoV2 main protease [21]. The study found that 14 ligands, including Andrographolide, can be considered as potential candidates for COVID-19 drugs. A study evaluated the in silico (molecular docking) characteristics of active compounds available in *Rosmarinus officinalis* (RM) and compared its biological effect with remdesivir and favipiravir as positive compounds based on docking properties [28]. The results showed that both selected compounds were much stronger in inhibition of the studied proteins compared with remdesivir and favipiravir. Based on the combined scores in binding affinity, the drug-likeness properties of the ligands, RM active compounds probably have

the therapeutic efficacy against covid-19 virus [28].

Finally, a study analyzed the binding affinity of four flavonoids screened against Mpro protein of SARS-CoV-2 by PyRx virtual screening tool and also validated the results with Lig-Plot Plus [29]. Rutin was found to have the highest binding affinity compared to Lopinavir with the Mpro protease, followed by chlorogenic acid, quercetin, and caffeic acid. The study concludes that Rutin present in the integrant of seeds shows the highest potentiality for acting as an inhibitor of the main protease enzyme. In summary, these studies suggest that andrographolide, withaferin-a, withanone, withanoside-iv, withanoside-v, and rutin are potential candidates for covid-19 drugs.

4 Conclusions

Based on the results of Molecular Docking simulation, secondary metabolites from the sambiloto plant (*A. Peniculata*) have been demonstrated to inhibit the activity of Covid-19 in humans through the Mpro receptor, as observed from the level of binding affinity generated. The results of Molecular Docking simulation showed that the affinity values of the test ligands were lower than the standard ligand, indicating that the test ligands had strong binding to the Mpro receptor of Covid-19. The test ligand with the highest affinity value was Andrographolide at -6.6 kcal/mol, while the ligand with the lowest affinity value was bisandrographolide at -8.5 kcal/mol. The analysis of interactions between the secondary metabolites from the sambiloto plant (*A. Peniculata*) and active residues revealed the presence of 61 hydrogen bonds from the 14 test ligands, as well as 4 hydrogen bonds in the standard ligand with varying bond distances.

5 Declarations

5.1 Authors contribution

Netty Ino Ischak: Conducted the literature review, designed the research methodology, and collected the data.

Akram La Kilo: Contributed to the conceptualization of the study, provided critical insights during the research process, and assisted in manuscript writing.

Dandi Saputra Halidi: Assisted in data collection and data validation, conducted experiments, and contributed to the interpretation of findings.

La Ode Aman: Provided expertise in the specific field of study, reviewed and revised the manuscript for intellectual content, and ensured the accuracy of the scientific information.

Jafar La Kilo: Assisted in data collection and data validation, conducted experiments, and contributed to the interpretation of findings.

Weny J.A Musa: Analyzed and interpreted the data and contributed to the discussion of results.

5.2 Funding

This research was not funded by any institution.

5.3 Conflict of Interest

The authors declare no conflict of interest in relation to this research study. They have no financial or personal relationships that could potentially bias the findings or interpretations presented in this paper. The research was conducted objectively and independently, without any external influences or competing interests.

6 References

- [1] M. Suciady, M. Meiliana, and D. N. Hendryanti, "Studi Literatur: Potensi Tanaman Herbal Indonesia sebagai Imunostimulan dan Anti-stress untuk Pencegahan Covid-19 Berbasis Evidence-based Analysis," *Prax. J. Sains, Teknol. Masy. dan Jejaring*, vol. 4, no. 1, p. 90, 2021, doi: 10.24167/praxis.v4i1.3607.
- [2] D. Kc, "Antiviral properties of medicinal plants of human diseases," *Int. J. Chem. Stud.*, vol. 8, pp. 2922–2924, 2020.
- [3] A. Devidas, "Investigation of Antiviral Properties of Medicinal Plant Extracts Research," 2014.
- [4] P. O. Oladosu, N. Moses, O. P. Adigwe, and H. O. Egharevba, "Potentials of Medicinal Plants with Antiviral Properties: The Need for a Paradigm Shift in Developing Novel Antivirals Against COVID-19," *J. Adv. Med. Med. Res.*, 2021.
- [5] B. Pujiasmanto and I. R. Manurung, "Identification of Sambiloto agroecology as a basis for utilization and conservation of germplasm," *IOP Conf. Ser. Earth Environ. Sci.*, vol. 1016, 2022.

- [6] A. F. Shofa, T. Alam, and N. Nuralih, "Uji Aktivitas Sitotoksik Ekstrak Polar, Semipolar, dan Non-Polar Daun Sambiloto (*Andrographis paniculata*) terhadap Sel Kanker Hati (HepG2)," *J. Kefarmasian Indones.*, 2022.
- [7] T. J. E. Tarigan *et al.*, "Effects of Sambiloto (*Andrographis paniculata*) on GLP-1 and DPP-4 Concentrations between Normal and Prediabetic Subjects: A Crossover Study.," *Evid. Based. Complement. Alternat. Med.*, vol. 2022, p. 1535703, 2022, doi: 10.1155/2022/1535703.
- [8] M. Sirat *et al.*, "The Effect of Supplementation of Sambiloto (*Andrographis paniculata*) Extract Through Drinking Water on Total Erythrocytes and Total Leucocytes of Broiler," *J. Ris. dan Inov. Peternak (Journal Res. Innov. Anim.)*, 2022.
- [9] M. Yolanda, S. B. Etika, and R. Riga, "KAJIAN FITOKIMIA DAN SIFAT ANTI BAKTERI JAMUR ENDOFITIK RS-1 PADA RANTING ANDROGRAPHIS PANICULATA (SAMBILOTO) DENGAN MEDIA PERTUMBUHAN BERAS MERAH," *EduMatSains J. Pendidikan, Mat. dan Sains*, 2022.
- [10] X. Y. Lim *et al.*, "*Andrographis paniculata* (Burm. F.) Wall. Ex Nees, Andrographolide, and Andrographolide Analogues as SARS-CoV-2 Antivirals? A Rapid Review," *Nat. Prod. Commun.*, vol. 16, 2021.
- [11] A. La Kilo, L. O. Aman, I. Sabihi, and J. La Kilo, "Studi Potensi Pirazolin Tersubstitusi 1-N dari Thiosemicarbazone sebagai Agen Antiamuba melalui Uji In Silico," *Indo. J. Chem. Res.*, vol. 7, no. 1, pp. 9–16, Jul. 2019, doi: 10.30598/ijcr.2019.7-akr.
- [12] N. I. Ischak, L. O. Aman, H. Hasan, A. La Kilo, and A. Asnawi, "In silico screening of *Andrographis paniculata* secondary metabolites as anti-diabetes mellitus through PDE9 inhibition," vol. 18, no. February, pp. 100–111, 2023, doi: 10.4103/1735-5362.363616.
- [13] Z. R. Mochamad, *Universitas indonesia penambatan molekuler beberapa senyawa xanton dari tanaman*. 2010.
- [14] R. Lelita, R. Gunawan, and W. Astuti, "Studi Docking Molekular Senyawa Kuersetin, Kalkon dan Turunannya Sebagai Inhibitor Sel Kanker Payudara MC-7 (Michigan Cancer Foundation-7)," *J. At.*, vol. 2, no. 2, pp. 190–196, 2017.
- [15] R. Rustaman, A. Mutalib, R. E. Siregar, and others, "Simulasi Doking Antibodi Monoklonal Chimeric dan Humanized dengan Reseptor HER-1 dan HER-2," *Indones. J. Appl. Sci.*, vol. 1, no. 1, 2011.
- [16] Y. K. Salimi, L. Ode, Z. Wathoni, and N. Ino, "Jurnal Kimia Sains dan Aplikasi Screening of Secondary Metabolite Compounds of Gorontalo Traditional Medicinal Plants Using the In Silico Method as a Candidate for SARS-CoV-2 Antiviral," vol. 25, no. 10, pp. 382–393, 2022.
- [17] Suharna, "Studi In Silico Senyawa Turunan Flavonoid Terhadap Penghambatan Enzim Tironase," *Skripsi*, p. 69, 2012.
- [18] N. I. Ischak and D. N. Botutihe, "Preliminary Study of Clinical Antidiabetic Activity of Salam Leaves (*Eugenia Polyantha*) and Sambiloto Leaves (*Andrographis Paniculata*) in Type 2 Diabetic Patients," *IOP Conf. Ser. Earth Environ. Sci.*, vol. 589, no. 1, 2020, doi: 10.1088/1755-1315/589/1/012034.
- [19] Z. Jin *et al.*, "Structure of Mpro from SARS-CoV-2 and discovery of its inhibitors," *Nature*, vol. 582, no. 7811, pp. 289–293, 2020, doi: 10.1038/s41586-020-2223-y.
- [20] F. J. Kelutur, "Sterol Constituents of Sea Fan (*Gorgonia mariae*) as Potential Candidates of MPro Protein SARS-CoV-2 Inhibitor: in silico Study," *Indo. J. Chem. Res.*, 2022.
- [21] A. Mishra, Y. Pathak, G. Choudhir, A. Kumar, S. K. Mishra, and V. N. Tripathi, "Abstract 712: Anticancer natural compounds as potential inhibitors of novel coronavirus (COVID19) main protease: An in-silico study," *COVID-19 and Cancer*, 2021.
- [22] A. Agusta, D. Wulansari, Praptiwi, A. Fathoni, L. Oktavia, and A. P. Keim, "Papuacerdrus papuana (f. Muell) h.l.li, A NEW SOURCE FOR TWO BIOACTIVE DITERPENES: FERRUGINOL AND transCOMMUNIC ACID THAT VIRTUALLY ACTIVE AGAINST SARS-COV-2," *RASAYAN J. Chem.*, 2022.
- [23] M. F. U. Rehman *et al.*, "Effectiveness of Natural Antioxidants against SARS-CoV-2? Insights from the In-Silico World.," *Antibiot. (Basel, Switzerland)*, vol. 10, no. 8, Aug. 2021, doi: 10.3390/antibiotics10081011.
- [24] M. M. Al-Sanea *et al.*, "Strawberry and Ginger Silver Nanoparticles as Potential Inhibitors for SARS-CoV-2 Assisted by In Silico Modeling and Metabolic Profiling.," *Antibiot. (Basel, Switzerland)*, vol. 10, no. 7, Jul. 2021, doi: 10.3390/antibiotics10070824.
- [25] P. Khanal *et al.*, "Combination of system biology to probe the anti-viral activity of andrographolide and its derivative against COVID-19.," *RSC Adv.*, vol. 11, no. 9, pp. 5065–5079, Jan. 2021, doi: 10.1039/d0ra10529e.
- [26] M. Nazari, M. Nazari, S. P. Arabani, and M. P. Nazarii, "Anti-Inflammation Prediction of Orthosiphon Stamineus Extract Against Covid19 (In Silico Study)," *Int. J. Eng. Technol. Sci.*, 2021.
- [27] R. S. Kalra *et al.*, "COVID19-inhibitory activity of withanolides involves targeting of the host cell surface receptor ACE2: insights from computational and biochemical assays.," *J.*

- Biomol. Struct. Dyn.*, vol. 40, no. 17, pp. 7885–7898, Oct. 2022, doi: 10.1080/07391102.2021.1902858.
- [28] N. Vm, “Anti-Inflammation Effects of Rosmarinus Officinalis Extract Against Covid19 Virus (In Silico Study),” *Bioequivalence \& Bioavailab. Int. J.*, 2021.
- [29] G. V. S. Kumar, R. Manivannan, and B. Nivetha, “In Silico Identification of Flavonoids from Coriandrum sativum Seeds against Coronavirus Covid-19 Main Protease,” *J. Drug Deliv. Ther.*, 2021.